Chapter 25

Density fronts and river plumes

25.1 Test case *river*

25.1.1 Description of the problem and model setup

Salinity fronts due to the fresh water input by river discharges are frequently occurring features in coastal areas and estuaries. The cross-frontal density gradients create the well-known estuarine circulation (see e.g. Heaps, 1972; Garvine, 1974; Officer, 1976) consisting of a surface outflow, a bottom inflow and downwelling motions at the front. The aim of test case ***river*** is to simulate the circulation and the evolution of a tidally modulated estuarine front and to analyse the influence of different schemes implemented in the program.

The problem is simplified by considering a non-rotating channel of uniform depth with open ends. Lateral effects are ignored. The channel length and depth are taken as 140 km and 20 m respectively. The initial position of the front is represented through the following distribution shown in Figure 25.1a:

$$\begin{array}{lll} S = 30 & \text{if} & x \leq 25 \\ S = \frac{1}{4}(x-25)+30 & \text{if} & 25 < x < 45 \\ S = 35 & \text{if} & x \geq 45 \end{array} \tag{25.1}$$

where S is the salinity in PSU and x the distance from the left boundary of the channel in km.

A tidal forcing is imposed by specifying the elevations and normal transports at the left boundary in harmonic form:

$$\zeta = A\cos(\omega t + \pi/2)\,, \quad U = c\zeta \tag{25.2}$$

where $c = \sqrt{gH}$ is the barotropic wave speed, H the water depth, U the depth-integrated current, $\omega = \pi/6$ rad/h the S_2 semi-diurnal frequency and

Table 25.1: Settings of the model switches for the ***river*** experiments. A "-" means that the value of the switch is irrelevant.

switch	***A***	***B***	***C***	***D***
iopt_adv_2D	1	1	1	3
iopt_adv_3D	1	1	1	3
iopt_vdif_coef	3	2	2	3
iopt_turb_alg	-	1	3	-

A the forcing amplitude taken as 0.8 m. At the right boundary, the normal gradient of the incoming Riemann variable R_- is assumed to vanish, i.e. $\partial R_-/\partial x = 0$. This allows the tidal wave to propagate freely from left to right. Since salinity remains vertically and horizontally homogeneous near the channel ends during the entire simulation, a zero normal gradient condition is selected for salinity at the two open boundaries.

The tidal current field within the simulated domain is initialised by splitting the simulation in two phases. During a first spin-up phase of 2 days the model is run without salinity. The salinity front is introduced at the start of the second run which takes 3 days.

25.1.2 Experiments and output parameters

Four experiments have been setup. The first three show the influence of the turbulence scheme while the fourth is intended to test the role of the advection scheme for momentum.

A **:** upwind scheme for momentum advection, default scheme for turbulence

B **:** Paconowski-Philander algebraic scheme for turbulence, upwind scheme for momentum advection

C **:** a flow-dependent algebraic scheme for turbulence, upwind scheme for advection of momentum

D **:** default scheme for turbulence, TVD scheme for the advection of momentum.

In all experiments the TVD scheme is applied for salinity. The values of the model switches, used for setting up each experiment are given in Table 25.1.

The final run is performed for 6 tidal cycles. The evolution of the front and the current field is shown in Figures 25.1b–f for the last cycle and the scheme ***A*** at intervals of 3 hours. Use is made of the program's utility for

making an harmonic analysis. Residuals, amplitudes and phases of the current and salinity are calculated by the program using a daily period. The distributions of the residual fields, obtained with scheme ***A***, are plotted in Figures 25.2a–c at daily intervals. The results for the last day are compared with those obtained for the other three experiments in Figures 25.2d–f. The non-analysed distributions of current and salinity at the end of the simulation are compared for the four experiments in Figures 25.3a–d. Note that the lowest 8 meters have been omitted in Figures 25.1 and 25.3. The time evolution of the position of the surface front, measured by the parameter hfront (see below), is displayed in Figure 25.4 for the four experiments.

The following output parameters are defined:

hfront The distance from the left boundary of the point where the front, measured by the 34 PSU contour line, outcrops the surface.

pdep The depth of the halocline measured 5 km to the left of the surface front. This is determined as the depth in m of the point where the salinity first equals 34.5 PSU.

hgrad This parameter measures the strength of the horizontal salinity gradient below the surface layer and is defined as the maximum value of $|dS/dx|$ in PSU/km along a layer halfway between the surface and the bottom. Note that the initial value, according to (25.1), is given by 0.25 PSU/km.

vgrad This parameter measures the sharpness of the halocline and is defined as the maximum value of $|dS/dz|$ in PSU/m along a vertical profile at 5 km to the left of the surface front.

The following harmonic parameters are defined at a location in the mid of the channel:

sures Residual value of the surface current in m/s.

suamp Amplitude of the surface current in m/s.

supha Phase of the surface current in degrees.

bures Mid-depth value of the residual current in m/s.

buamp Mid-depth amplitude of the current in m/s.

bupha Mid-depth phase of the current in degrees.

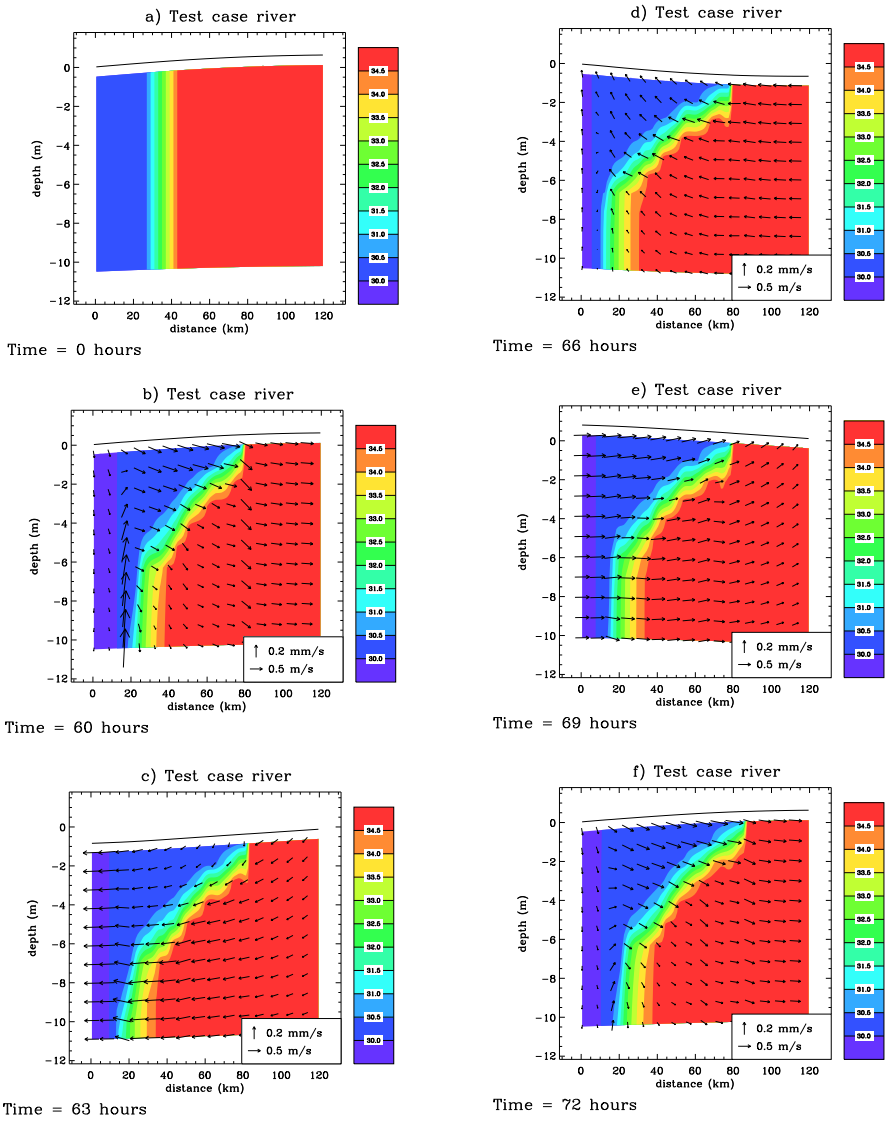

Figure 25.1: Test case ***river***. Initial position of the salinity front (a). Evolution of the current and salinity fields during the last tidal cycle for experiment ***A*** at intervals of 3 hours (b–f).

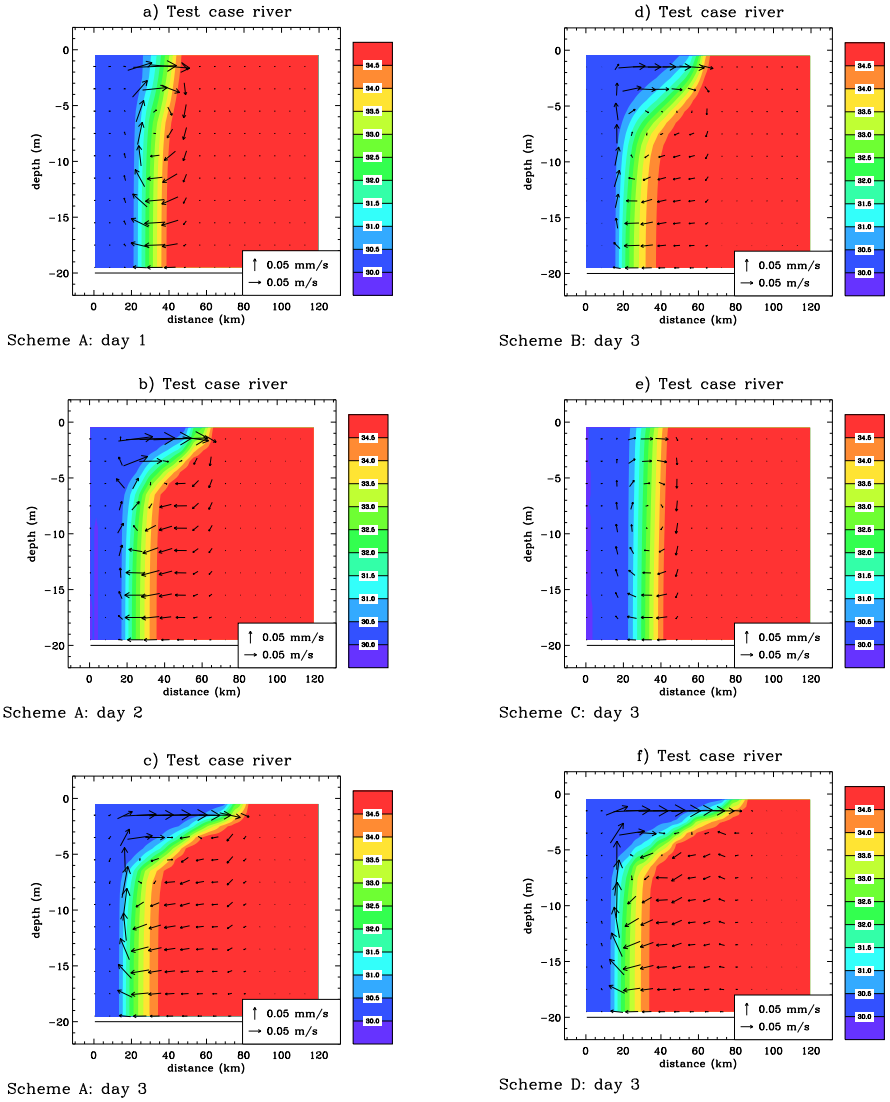

Figure 25.2: Test case ***river***. Residual salinity and current field for experiment ***A*** analysed for day 1 (a), 2 (b), 3 (c). The same now for day 3 and experiment ***B*** (d), ***C*** (e), ***D*** (f).

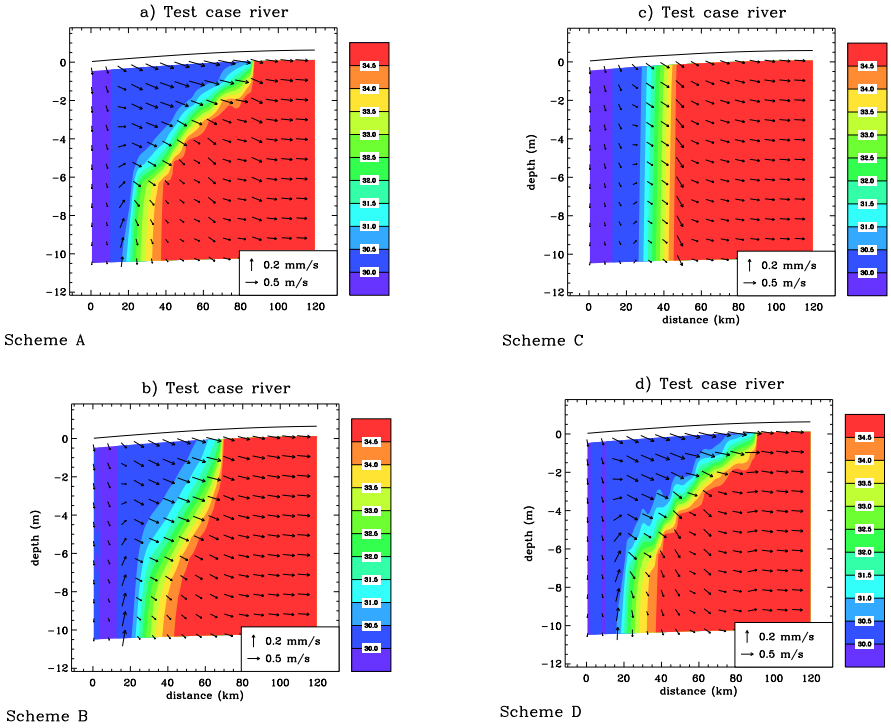

Figure 25.3: Test case ***river***. Distributions of current and salinity at the end of the simulation for experiment ***A*** (a), ***B*** (b), ***C*** (c), ***D*** (d).

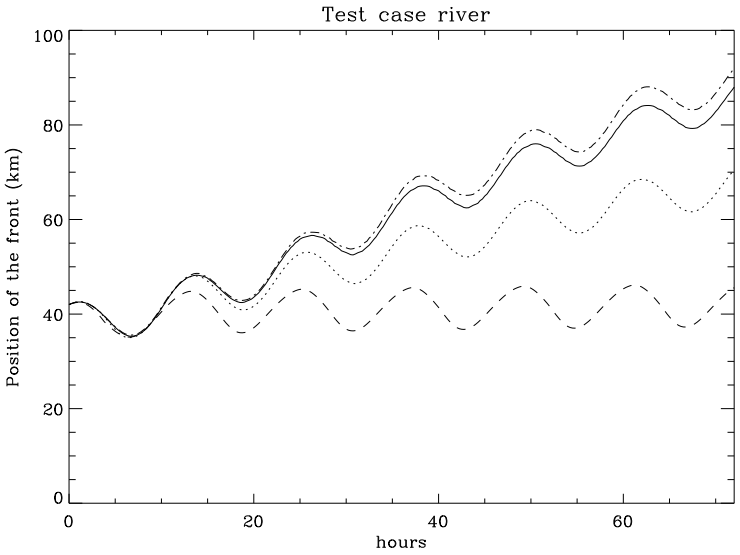

Figure 25.4: Test case ***river***. Time series of the distance to the left boundary of the point where the front outcrops the surface for experiment ***A*** (solid), ***B*** (dots), ***C*** (dashes), ***D*** (dash-dots).

25.1.3 Results

The evolution of the frontal system for experiment ***A*** can be described as follows. The initial configuration represents a non-equilibrium state. Although the model setup is different from the ***seich*** problem, where turbulent diffusion is absent, there is some similarity. A circulation is generated with a surface flow to the right, a bottom flow to the left, downwelling at the right edge and upwelling at the left edge of the front. Contrary to the ***seich*** test, the current is generated by a balance between the baroclinic pressure gradient and the vertical diffusion term, induced by tidal friction (Officer, 1976). The initial evolution therefore consists of a slight displacement of the surface front to the right and the bottom front to the left. The circulation pattern is modulated by the tide so that at the end of the cycle the front almost returns to its original position. The turbulent diffusion term, however, varies with the tide. This means that turbulence is suppressed during the phases where the current reverses sign and the shear is low. At that time the balance in the momentum equation is now mainly between the baroclinic pressure and inertia terms as in the ***seich*** problem giving a net displacement of the surface layer to the right. The surface and bottom layer are separated by a halocline of increasing strength. The vertical stratification

reduces the turbulence even further and enhances the motion of the surface layer to the right. Figure 25.4 shows that the front moves with an almost uniform mean speed on which tidal modulations are superimposed. As the front moves further out downwelling at the front due to frontal convergence, first increases and then decreases. The main aspects of the physical analysis can be observed in Figures 25.1b–f and Figure 25.4.

The results for the other three experiments can be summarised as follows:

- Experiment ***B*** uses the Paconowski-Philander scheme. Contrary to the default scheme, turbulence is less reduced in the case of a strong stable stratification. The result is a more diffusive halocline and a slower outward expansion of the front.

- The flow-dependent scheme of experiment ***C*** is much more diffusive. The front returns to its initial position after each cycle so that no halocline forms and the front does not expand outwards. The test clearly shows the importance of the turbulence scheme in the simulation of estuarine fronts.

- Experiment ***D*** uses the same turbulence model as scheme ***A*** but advects the current with the less diffusive TVD scheme. The results are an increase of the inertial force and horizontal density gradient and a larger expansion speed of the surface front.

- In experiment ***D***, the upwelling and downwelling motions are modulated by the tide which generates in combination with the vertical density gradient, an internal tide. The wavelength of the tide is ~ 5 km. Only the TVD scheme is capable of representing this internal tide. This indicates again the importance of adequate schemes for advection and turbulence to model frontal processes.

25.2 Test case *plume*

25.2.1 Description of the problem and model setup

In the test case ***river***, the evolution of a salinity front was simulated within a narrow non-rotating channel. When a river discharges fresh water into the open sea, rotational effects become important and the problem becomes three-dimensional. The formation and evolution of river plumes has been examined numerically by e.g. Chao & Boicourt (1986); Chao (1988); Kourafalou *et al.* (1996) in the absence of tides and by Ruddick *et al.* (1995) who simulated the tidally modulated plume of the river Rhine. The general picture,

emerging from these studies, is that the fresh water released at the river mouth, first expands seawards and then turns anticyclonically (i.e. to the right looking seawards in the northern hemisphere). Before reaching the coast again, the plume water deflects in the cyclonic sense forming a buoyancy driven coastal jet. The general form of the plume then consists of an anticyclonic bulge with a coastal plume to the right (in the northern hemisphere). The width of the plume is of the order of the baroclinic Rossby radius (∼5–10 km).

The aim of the test case ***plume*** is to simulate the evolution of a tidally modulated river plume using the idealised conditions of a uniform water depth and no wind forcing. The computational domain has the form of a rectangle enclosed by a coastal (solid) boundary and three open sea boundaries. For convenience, the former will be denoted by the southern boundary, the latter by the western, eastern cross-shore boundaries and the northern alongshore boundary. The basin has a length of 120 km, a width of 40 km and a depth of 20 m. The horizontal resolution is 1 km and 20 levels are used in the vertical. The area is filled initially with seawater having a uniform salinity of 33 PSU. The simulations are performed in Cartesian coordinates with the x-axis taken alongshore and the y-axis across-shore (see Figure 25.5).

Tidal forcing is imposed in the form of a frictionless Kelvin wave entering at the western boundary and propagating along the coast (Ruddick *et al.*, 1995). The incoming Riemann variable, specified at the western boundary, then takes the form

$$\zeta = Ae^{-y/c}\cos(\omega t)\,, \quad U = c\zeta \tag{25.3}$$

where the Coriolis frequency is evaluated at a latitude of 52°, ω is the M_2 tidal frequency, $A = 0.8$ m and U, c, ζ are as before the depth-integrated alongshore current, the barotropic wave speed and the surface elevation. The amplitude of the wave decreases exponentially with distance to the coast with a decay scale given by the barotropic Rossby radius $c/f \simeq 120$ km.

The characteristic method with a zero normal gradient condition for the incoming characteristic is selected at the eastern and northern boundaries. The condition is justified by the fact that the width of the basin is much smaller than the external Rossby radius c/f.

In a first phase the model is run for a period of two days (almost four tidal cycles) without any stratification to initialise the current field and the sea surface elevation. At the start of the the final run fresh water of 10 PSU is released through an inlet at the southern boundary located 25.5 km from the western boundary. The evolution of the plume is then simulated for a period of three days. The procedures are the same as outlined in Section 25.1.1 for the ***river*** test case.

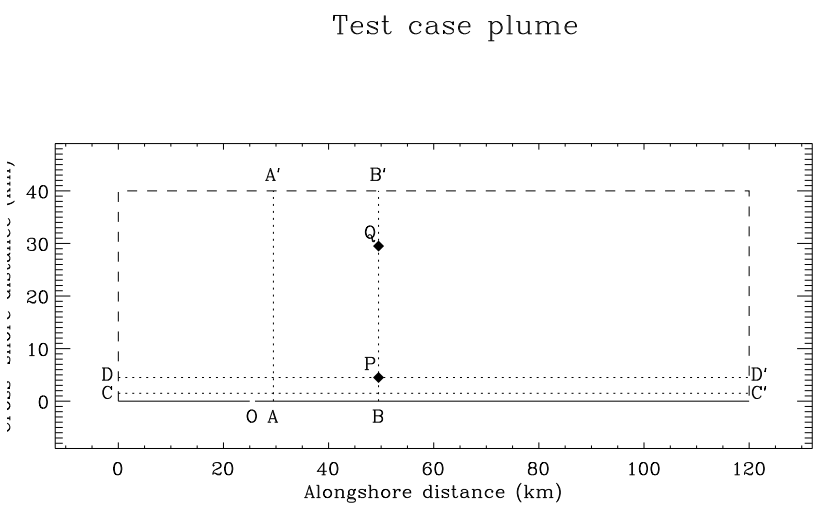

Figure 25.5: The computational domain for the test case ***plume***. The solid line(s) indicate the coastal (southern) boundary, the dashed lines the open sea boundaries and the dotted lines the two cross-shore transects AA' ($x = 30$), BB' ($x = 50$) and the two alongshore transects CC' ($y = 2$) and DD' ($y = 5$). The inlet is located at O. Points P and Q are used for the evaluation of a number of output parameters (see text).

Since the value of ζ is unknown at the river mouth, the open boundary condition at the inlet is no longer defined in terms of the incoming Riemann variable but by specifying the cross-shore component of the depth-integrated current. This is given as the sum of a residual value, representing the river discharge, and a tidal component

$$V = Q_d/W + A_r H \cos(\omega t - \varphi_r) \tag{25.4}$$

where $Q_d = 1500$ m^3/s is the river discharge, $W = 1$ km the width of the inlet and $A_r = 0.6$ m/s the amplitude of the tidal current at the mouth of the river. The phase φ_r is determined by

$$\varphi_r = \omega D_r/c - \pi/2 \tag{25.5}$$

where $D_r = 25.5$ km so that D_r/c represents the time travelled by the Kelvin wave from the western boundary to the river mouth. Observations in the

Rhine plume show that the alongshore and cross-shore component are in anti-phase which explains the use of the factor $\pi/2$.

In addition to the previous conditions for the 2-D mode, open boundary conditions have to be imposed during the final run for the horizontal baroclinic currents (δu, δv)[1] and the salinity S. At the open sea boundaries a zero normal gradient (default) condition is taken for all quantities. In the case of salinity this procedure is a reasonable approximation since the plume never intersects the western and northern boundary while the cross-boundary gradient in the non-tidal case (experiment ***G*** below) is much smaller than the along-boundary gradient at the eastern boundary.

The default conditions are no longer applicable at the river mouth where δv and S are specified in the form of a two-layer stratification

$$\begin{array}{ll} S = 10\,,\ \delta v = 0.6 & \text{if} \quad z > -\delta \\ \delta v = -0.2 & \text{if} \quad -H \leq z \leq -\delta \end{array} \tag{25.6}$$

where $\delta = 5$ m is the specified depth of the plume layer at the mouth. In this way fresh water is released through the surface layer whereas saltier seawater flows into the estuary through the bottom layer. A zero gradient condition is applied for salinity in the bottom layer.

25.2.2 Experiments and output parameters

Although the ***plume*** problem is a valuable test to examine the role of different physical forcing mechanisms (bathymetry, tides, wind, ...) on the plume structure, the intention here is to test some of the schemes implemented in the program[2]. Seven experiments are defined testing the role of the different formulations for horizontal diffusion and different boundary conditions.

A **:** Uses default values and model setup.

B **:** As experiment ***A*** now using the upwind scheme for the advection of momentum.

C **:** As experiment ***B*** now with horizontal diffusion enabled using the Smagorinsky formulation.

D **:** As experiment ***B*** now with horizontal diffusion enabled and using the uniform values $\nu_H = \lambda_H = 100$ m^2/s for the horizontal diffusion coefficients.

[1] The velocity deviations are defined as the current minus its depth-averaged value.

[2] The influence of winds on plume evolution are considered in test case ***rhone*** discussed in the next section.

E* :** As experiment ***D but the boundary condition (25.3) is replaced by a condition for the surface elevation only:

$$\zeta = Ae^{-fy/c}\cos\omega_2 t \tag{25.7}$$

F* :** As experiment ***D but the boundary condition (25.3) is replaced by a condition for the depth-integrated current only:

$$U = cAe^{-fy/c}\cos\omega_2 t \tag{25.8}$$

G* :** As experiment ***A but without tidal forcing which means that condition (25.3) is replaced by a zero gradient condition at the western boundary and A_r is set to zero in the condition (25.4) at the inlet.

A series of figures have been prepared for this test case. The intention is not only to examine the structure and the evolution of the river plume and to compare the different experiments, but also to illustrate how harmonic analysis can be applied to model results. The time evolution of the surface plume for experiment ***A*** is shown in Figures 25.6 during the third cycle at intervals of 3 hours. The residual salinity and current field obtained for the last 12 hours of the simulation are compared in Figures 25.7 for all experiments (except ***F*** which is similar to ***E***). The residual fields plotted in Figures 25.8a–b and 25.8c–d for experiments ***A*** and ***G*** are taken respectively along the transects AA' perpendicular and DD' parallel to the coast (see Figure 25.5 for a location of the transects). The time evolutions of plume width and length are compared in Figures 25.9 for several experiments. The first figure shows the plume width taken as the cross-shore distance of the 32 PSU contour line from the mouth, the second the length of the plume measured by the alongshore distance between the inlet and the point to the right along transect CC' where the salinity reaches a value of 32 PSU. Harmonically analysed values and current ellipse parameters for experiment ***A*** are displayed in Figures 25.10 (surface and bottom ellipticity), 25.11a–c (major axis of the tidal ellipse for the depth-averaged current and experiments ***A, E, F***) and 25.11d–f (amplitude of the surface elevation for the same experiments).

A series of output parameters are defined. The first four are evaluated at intervals of 6 hours. For a location of the transects and points see Figure 25.5.

hbulge The width of the plume bulge. This is measured by the maximum distance in km of the 32 PSU surface contour line from the coast.

hwidth The width of the coastal plume measured by the distance from the coast in km of the point where the 32 PSU surface contour line intersects the transect BB'.

pdep Depth of the surface plume at point P measured by the distance to the surface in m of the 30 PSU contour line.

hfront The length of the plume measured by the alongshore distance in km between the river mouth and the point where the 32 PSU surface contour line intersects the transect CC'.

A second series of parameters represent harmonically analysed values of the current and surface elevation and tidal ellipse parameters at the two points P and Q. The analysis is performed for the last 12 hours of the simulation.

sures
: Surface value of the residual u-current at P (m/s).

svres
: Surface value of the residual v-current at P (m/s).

selmaj
: Surface value of the tidal ellipse's major axis at P (m/s).

sellip
: Ellipticity of the surface ellipse at P.

bures
: Value of the residual u-current at P and 10 m depth (m/s).

bvres
: Value of the residual v-current at P and 10 m depth (m/s).

belmaj
: Value of the tidal ellipse's major axis at P and 10 m depth (m/s).

bellip
: Ellipticity of the tidal ellipse at P and 10 m depth.

dures
: Residual value of the depth-averaged u-current at Q (m/s).

duamp
: Amplitude of the depth-averaged u-current at Q (m/s).

dupha
: Phase of the depth-averaged u-current at Q (degrees).

zetres
: Residual surface elevation at Q (m).

zetamp
: Amplitude of the sea surface elevation at Q (m).

zetpha
: Phase of the sea surface elevation at Q (degrees).

The residual values for experiment ***G*** are obtained by taking averaged values over the last 12 hours.

25.2.3 Results

- Figures 25.6 clearly show how the plume evolves during a tidal cycle. At the time when the alongshore current reverses sign and the outflow reaches its maximum, a new blob of fresh water enters the basin, moving seawards. As the eastward directed tidal wave becomes stronger, the fresh water patch is deflected to the right. During this phase of the tide both the bulge and the coastal plume expand seawards. When the tidal current reverses sign again and turns to the west, the current inside the plume is first southeastwards pushing the bulge towards the coast and finally southwestwards reducing the extent of the bulge and the coastal plume. Since the tidal current enforces the anticyclonic motion inside the bulge, the results are similar to the ones obtained for non-tidal plumes. The main difference here is that the bulge and the coastal plume oscillate with the tide.

- After a few tidal cycles (Figures 25.7) the structure of tidal and non-tidal plumes are manifestly different. While in the latter case the transition between the bulge and the coastal plume is clearly observed, no clear distinction can be made in the former case. This effect is due to increased turbulent diffusivity which reduces the anticyclonic vorticity inside the bulge and the strength of the coastal current. The effect becomes more pronounced when more horizontal diffusion is introduced in the simulation either by using the upwind scheme for momentum advection or by adding horizontal diffusion terms in the momentum and salinity equations.

- The residual fields along the two transects AA' and DD' (Figures 25.8) show the presence of an estuarine-type circulation. In the cross-shore transect upwelling takes place at the coast while downwelling occurs at the edge of the plume by the convergence of the surface outflow current. A similar phenomenon is seen in the coastal jet where downwelling motions are created by the convergence of the coastal jet. In the case of a non-tidal plume the plume layer is shallower and the frontal

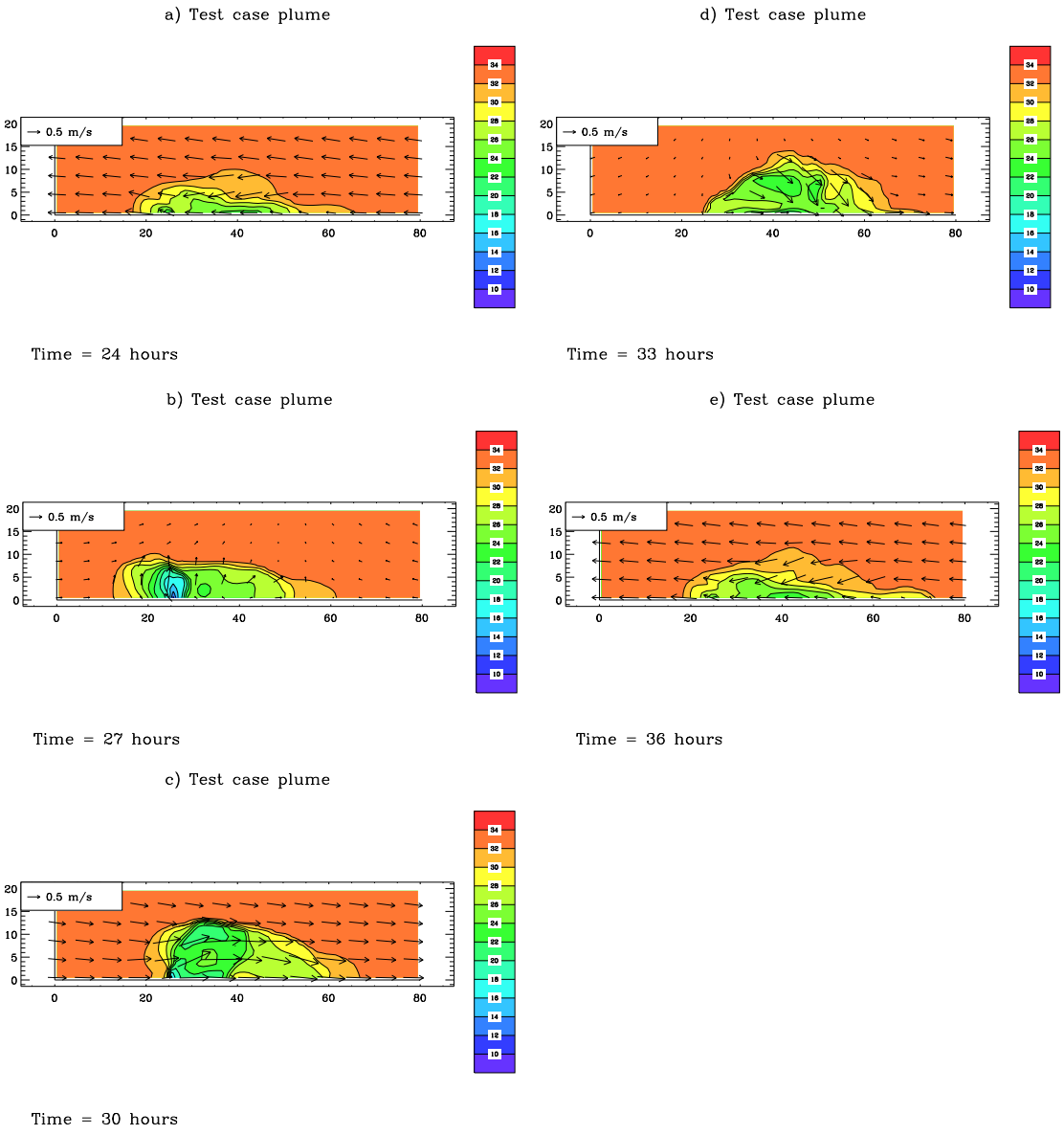

Figure 25.6: Test case ***plume***. Surface distributions of currents and salinity for experiment ***A*** at 24 h (a), 27 h (b), 30 h (c) 33 h (d), 36 h (e).

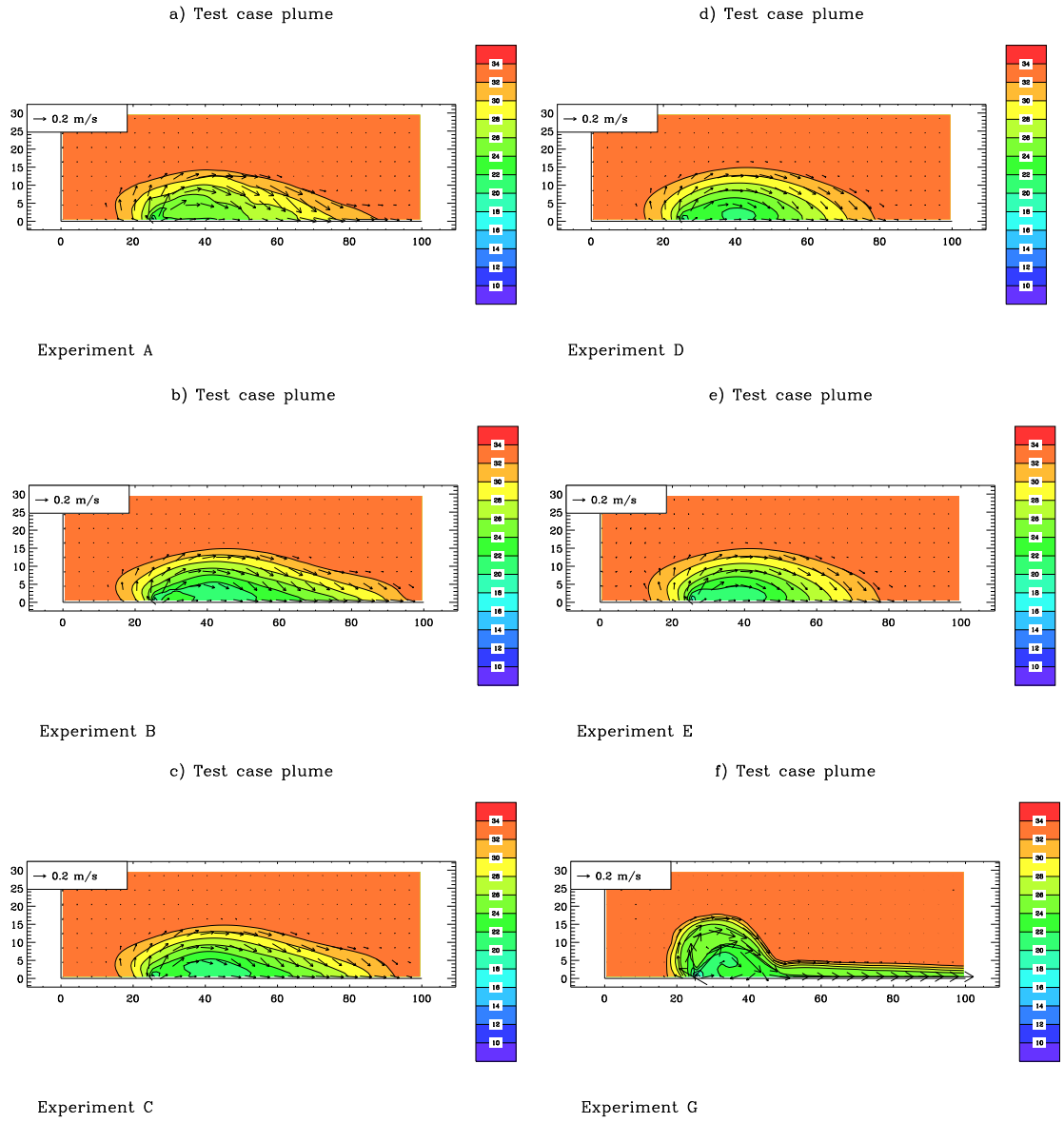

Figure 25.7: Test case ***plume***. Residual surface distributions of currents and salinity for the last tidal cycle and experiment ***A*** (a), ***B*** (b), ***C*** (c), ***D*** (d), ***E*** (e), ***G*** (f).

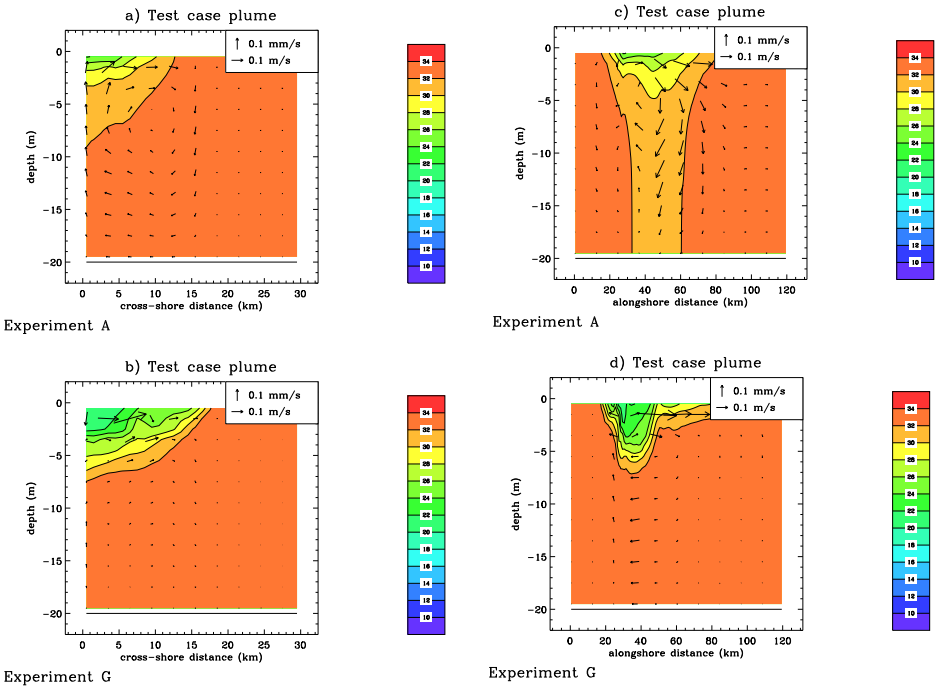

Figure 25.8: Test case ***plume***. Residual distributions of currents and salinity for the last tidal cycle along the cross-shore transect AA' for experiment ***A*** (a), ***G*** (b), and at the alongshore transect DD' for experiment ***A*** (c), ***G*** (d).

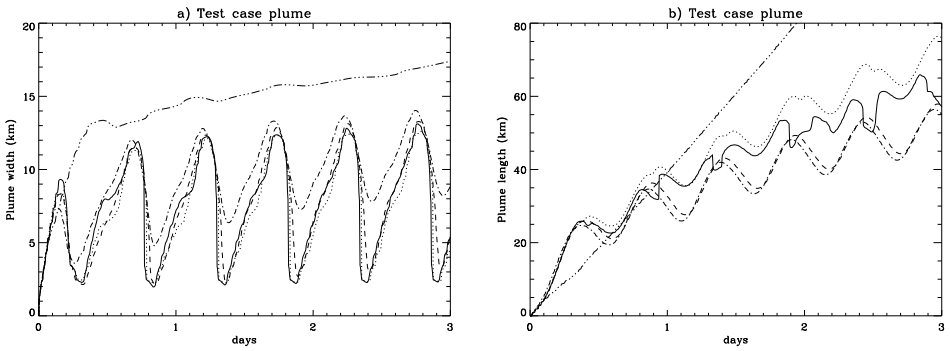

Figure 25.9: Test case ***plume***. Time series of the plume width taken as the cross-shore distance of the 32 PSU contour line from the mouth (a) and of the plume length at the transect CC' (b) for experiments ***A*** (solid), ***B*** (dots), ***D*** (dashes), ***E*** (dash-dots) and ***G*** (dash and 2 dots).

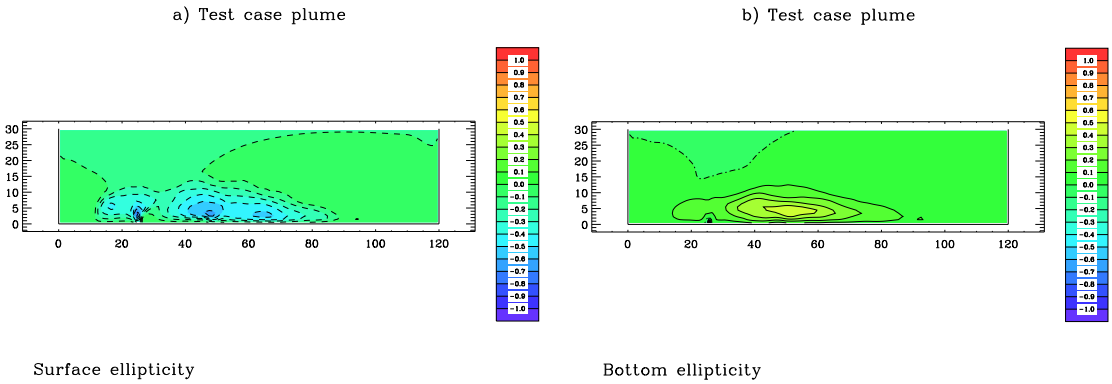

Figure 25.10: Test case ***plume***. Ellipticity of the tidal ellipses for experiment ***A***: surface (a) and bottom (b) distributions. Negative and positive values are drawn by dashed, respectively solid lines. The analysis is performed for the last tidal cycle.

gradients are stronger compared to the tidal case where turbulent diffusion increases the depth of the surface layer and reduces the vertical stratification.

- The oscillations of the plume shape induced by the tide are clearly observed in Figures 25.9. In the absence of tides the width of the bulge first grows in time levelling off after 10–12 hours which is comparable to the inertial period of $\sim$ 15 h. A somewhat similar behaviour can be deduced for the tidal case where the mean growth curve is strongly modulated by the tide. The length of the plume increases linearly in the non-tidal case. In the presence of tides the growth is strongly reduced as found previously and seems to decrease asymptotically. The experiments with horizontal diffusion show a slower growth of the coastal plume.

- The presence of a stratified surface layer has an important impact on the form of the tidal current. Outside the plume the current is rectilinear (zero ellipticity) while inside the plume the current rotates anticyclonically (negative ellipticity) in the surface and cyclonically (positive ellipticity) in the bottom layer. This is confirmed by observational data in the Rhine plume and the physical theory discussed in Visser *et al.* (1994).

- The amplitude of the depth-averaged tidal current measured by the

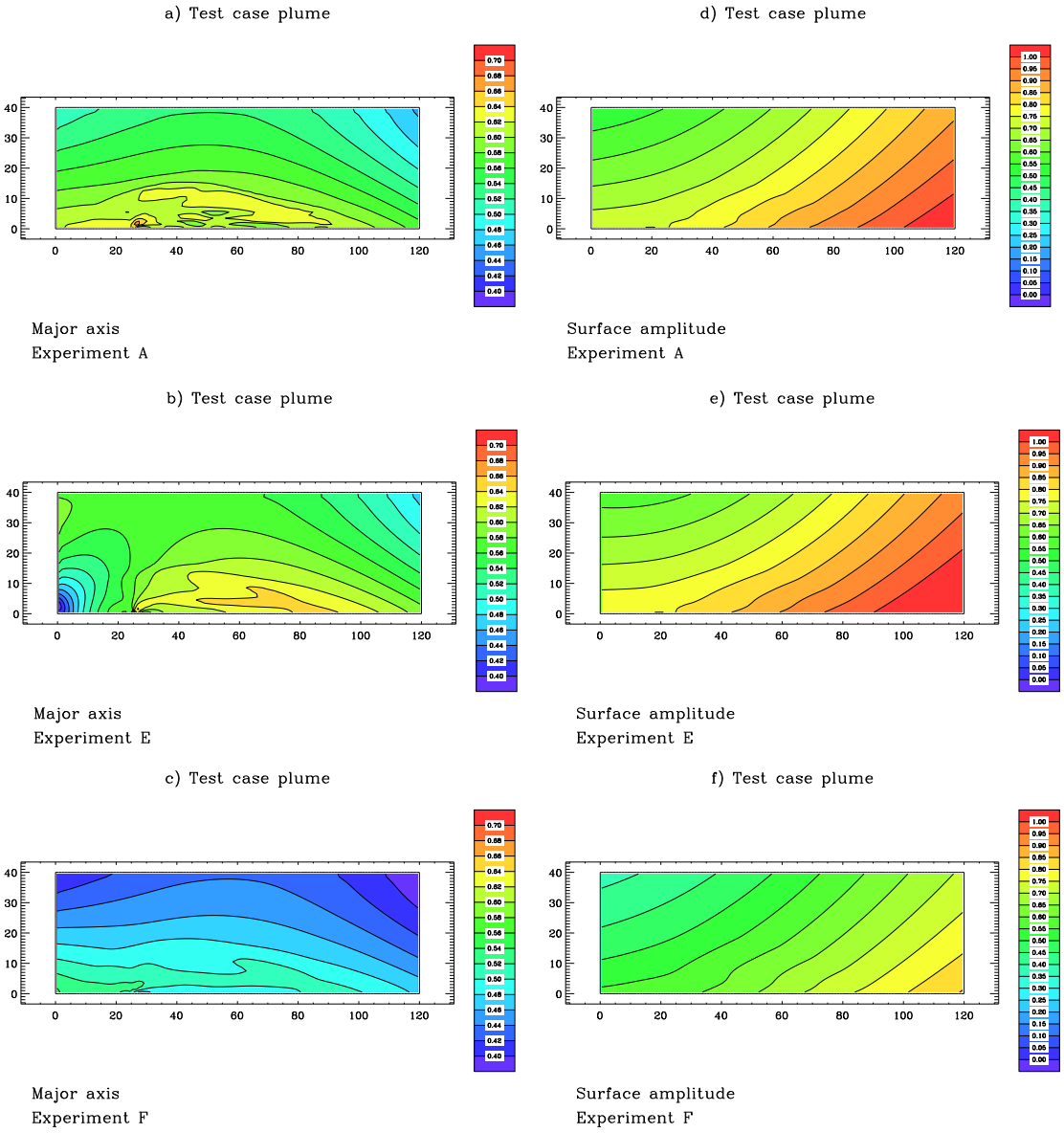

Figure 25.11: Test case ***plume***. Distributions of the major axis (m/s) of the tidal ellipse for the depth-averaged current and $\boldsymbol{A}$ (a), $\boldsymbol{E}$ (b), $\boldsymbol{F}$ (c) and of the M_2 surface elevation amplitude and $\boldsymbol{A}$ (d), $\boldsymbol{E}$ (e), $\boldsymbol{F}$ (f).

major axis of the tidal current is clearly stronger inside the plume due to the reduction of the turbulence and the bottom shear stress. No significant change is found for the amplitude of the surface elevation.

- Figures 25.11 compare the three different formulations for the tidal forcing at the western boundary, represented by experiments ***A***, ***E*** and ***F***. Although the results are qualitatively the same, there are important quantitative differences. On the other hand, the results shown in Figures 25.10, 25.11a and 25.11d are practically the same for experiments ***A***, ***B***, ***C*** and ***D*** suggesting that horizontal diffusion has no significant influence on the tidal currents (at least for this idealised test case).

25.3 Test case *rhone*

25.3.1 Description of the problem and model setup

The outflow of the Rhone river is located in the Gulf of Lions situated between $42^0 - 43^0 30' N$ and $3^0 - 6^0 E$. The bottom topography in most areas along the French coast, including the Rhone plume area, is characterised by a steep slope with depths increasing rapidly up to values of 1000 m at 20–50 km from the coast. Observations (Albérola *et al.*, 1995) and numerical simulations (Tsimplis *et al.*, 1995) indicate that tides are insignificant in most parts of the Western Mediterranean. This is even more the case in the Gulf of Lions where tidal amplitudes have values of only a few cm and tidal currents are extremely low (less than 0.1 cm/s). The ***rhone*** test case can therefore be considered as complementary to the ***plume*** case discussed in the previous section. The discharge of the Rhone river provides a major input of fresh water, nutrients, sediments and suspended material in the Gulf of Lions and even the Western Mediterranean. The drainage area is of the order of $\sim 10^5$ km^2. The mean river discharge is 1700 m^3/s with strong seasonal variations between $\sim$500 and $\sim$8000 m^3/s. The lowest and highest values occur in October and March–April.

The Rhone plume can be observed by infrared satellite images in the summer (winter) when the plume water is warmer (colder) than the ambient seawater of the Gulf of Lions. Demarcq & Wald (1984) used remote sensing to study the influence of the wind on the shape of the plume. In the absence of wind the plume is confined to the coast. The response of the plume to the wind is rapid and consists in a deflection of the plume to the right of the wind direction with an average angle of deflection of $\sim 50^0$. Northwesterly winds, which are typical for the winter regime, cause the plume to expand seawards with a tendency to detach from the coast. A southeasterly wind

on the other hand confines the plume even more to the coast while the fresh water spreads in eastward direction and may attain the Gulf of Fos.

The frontal boundary of a river plume is not only characterised by strong gradients of salinity but also by front convergence, i.e. a strong negative gradient of the current towards to the front. Forget *et al.* (1990) used a VHF radar technique to determine the plume boundary by measuring the current in the direction of the radar beam. The frontal boundary can easily be identified by a jump ($\sim$20 cm/s) in the current field. Inside the plume values of 50 cm/s were measured.

The river plume can be identified in the salinity field by two frontal regimes.When the low salinity water (10–15 PSU) of the Rhone river discharges into the the Gulf of Lions ($\sim$ 38 PSU), the fresh water spreads outwards in the form of a highly stratified ($\sim$10 PSU/m) surface layer with low turbulence and a thickness of a few meters, floating above a mixed bottom layer. Flow convergence occurs at the edge of the plume. This area, often visible by foam, has a width of only a few hundred meters and acts as a source for the accumulation of dissolved material, sediments and nutrients. At the lateral frontal boundary the horizontal gradient is of the order of 7 PSU/km. Salinity measurements in the Rhone plume are reported by e.g. Sournia *et al.* (1990); Naudin *et al.* (1992).

The domain of the simulations, covers the area between $43^0 05'$ – $43^0 30'$N and $4^0 07'$ – $5^0 28'$E. The X- and Y-axis are directed respectively along the West-East and South -North directions. The horizontal resolutions are given by $\Delta\phi = 30''$ in latitude and $\Delta\lambda = 45''$ in longitude which corresponds approximatively to a 1×1 km grid.

The bathymetry of the area is displayed in Figure 25.12. The estuary of the Rhone river is approximated by a straight channel having a width of 1 km and a length of 6.5 km (7 grid cells). Fresh water (salinity of 10 PSU) is discharged at the head of the channel. The bathymetry in front of the river mouth is characterised by a strong seaward bottom slope with a water depth increasing from 10 m at the mouth upto 100 m at distance of $\sim$10 km from the coast. The strongest gradient occurs within a distance of only 1 km from the mouth. To represent this effect in the model a seaward bottom slope is introduced inside the channel allowing the water depth to increase from 5 m at the head of the channel to 20 m at the mouth. Other areas of interest for the plume study are the Gulf of Fos, located at the East of the river mouth which is a shallow area with depths between 5 and 20 m, and the Camargue coast to the West where the water depth increases less rapidly with the distance to the coast.

The following setup is used:

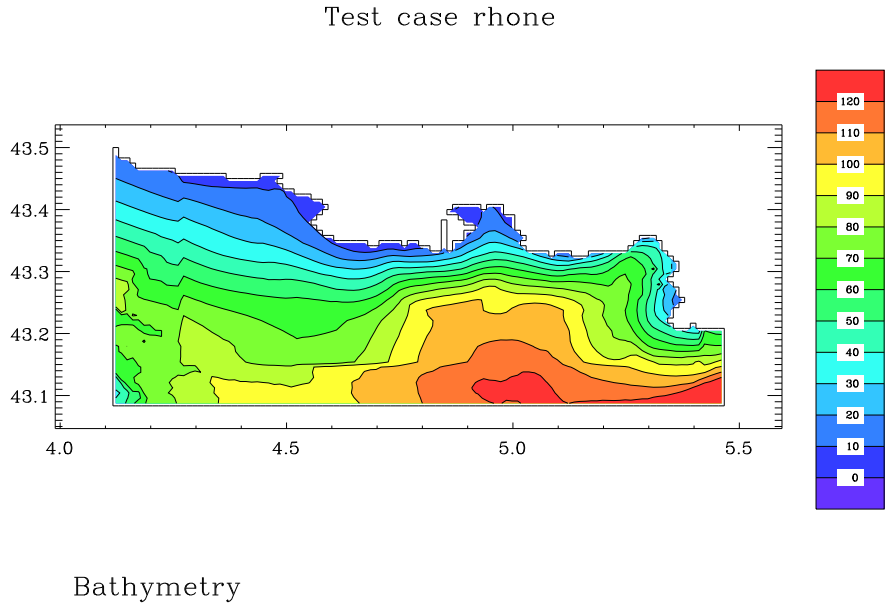

Figure 25.12: Bathymetry of the Rhone plume area.

- The TVD scheme is applied for all transport equations.
- The baroclinic pressure gradient is evaluated using the z-level scheme (iopt_dens_grad=2).
- Time steps are 10 s for the 2-D and 180 s for the 3-D mode and the simulations are performed for a period of 4 days.
- The simulations start with zero initial currents and a uniform salinity of 38.1 PSU.
- A zero normal gradient for the incoming Riemann characteristic is imposed at all open sea boundaries.
- The river discharge at the river mouth is taken as uniform in time and over the vertical which means that the baroclinic current at the mouth is set to zero. The salinity of the fresh water release is set to 10 PSU.

25.3.2 Experiments and output parameters

Seven experiments are defined. Except for ***C*** the aim is not to test numerical algorithms and schemes but to analyse the role of physical forcing parameters

like discharge rate and wind.

A : Standard run without wind and a discharge rate Q=1500 m^3/s.

B* :** As experiment ***A now using Q=6000 m^3/s.

C* :** As experiment ***A now using the Pacanowski-Philander algebraic turbulence scheme as defined in Section 4.4.2.1.

D* :** As experiment ***A with a wind speed of 6 m/s and a wind direction of 0 degrees (westerly wind).

E* :** As experiment ***D but now with a wind direction of 90 degrees (southerly wind).

F* :** As experiment ***D but now with a wind direction of 180 degrees (easterly wind).

G* :** As experiment ***D but now with a wind direction of 270 degrees (northerly wind) .

In all wind experiments the wind is set to zero during the first two days.

The following output parameters are defined

area34	Area (in km^2) where salinity is lower than 34 PSU.
area22	Area (in km^2) where salinity is lower than 22 PSU.
ekin	Volume integrated kinetic energy (10^9J).
epot	Volume integrated potential and internal energy (10^9J).
etot	Volume integrated total energy (10^9J).
bdissip	Volume integrated energy dissipation (10^6W).
enstr	Volume integrated vorticity (m^3/s^2) as defined by (23.14).
curmax	Maximum value of the horizontal current magnitude (cm/s).
wmax	Maximum value of the transformed vertical current (mm/s).
wmin	Minimum value of the transformed vertical current (mm/s).
d34max	Maximum distance (km) of the 34 PSU contour line from the coast.

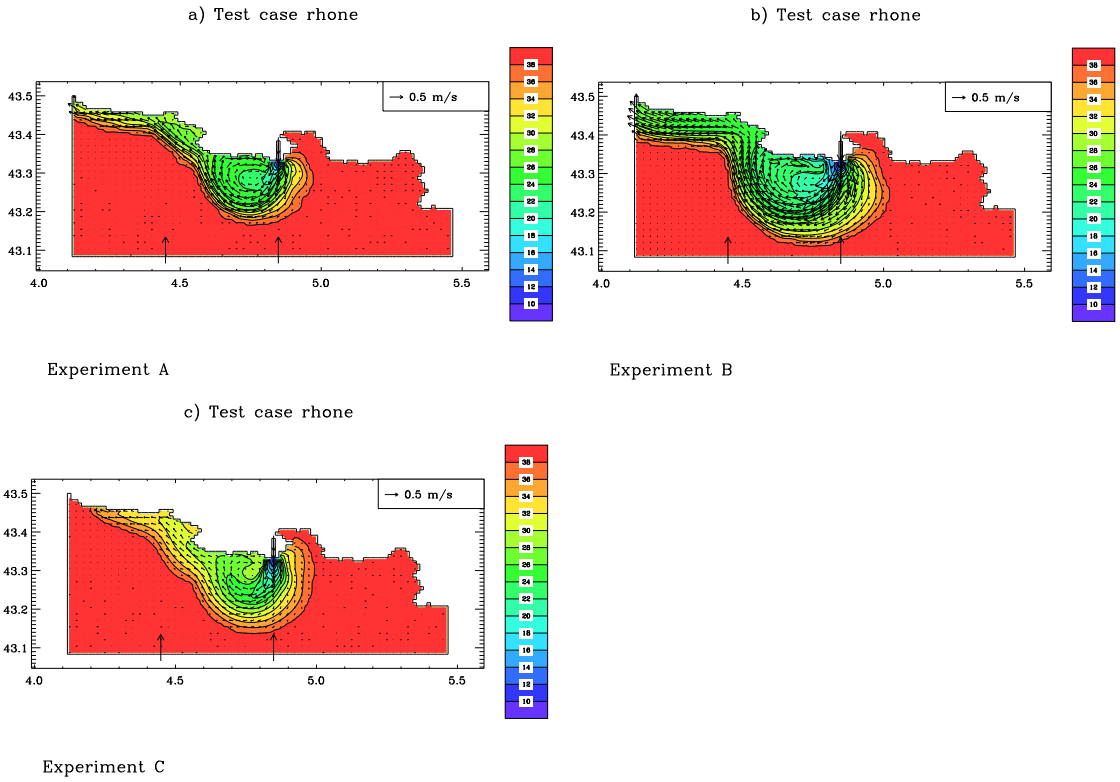

Figure 25.13: Test case ***rhone***. Surface distributions for salinity and currents for experiment ***A*** (a), ***B*** (b), ***C*** (c). The arrows on the southern boundary locate the positions of the South-North transects shown in Figures 25.14 and 25.15.

25.3.3 Results

The following series of figures are produced for all experiments at the end of simulation. Surface plume and currents are shown for all epxeriments in Figures 25.13 and 25.16, salinity and current distributions are displayed along different vertical transects in Figures 25.14, 25.15 and 25.17. Time series of the plume area, as defined by the test parameter area34 are displayed in Figures 25.18.

1. No wind experiments.

   - Experiment ***A*** shows the "traditional" evolution of a non-tidal plume at non-tropical latitudes (Figure 25.13a). The plume spreads outwards in offshore direction over a few kilometers, then turns

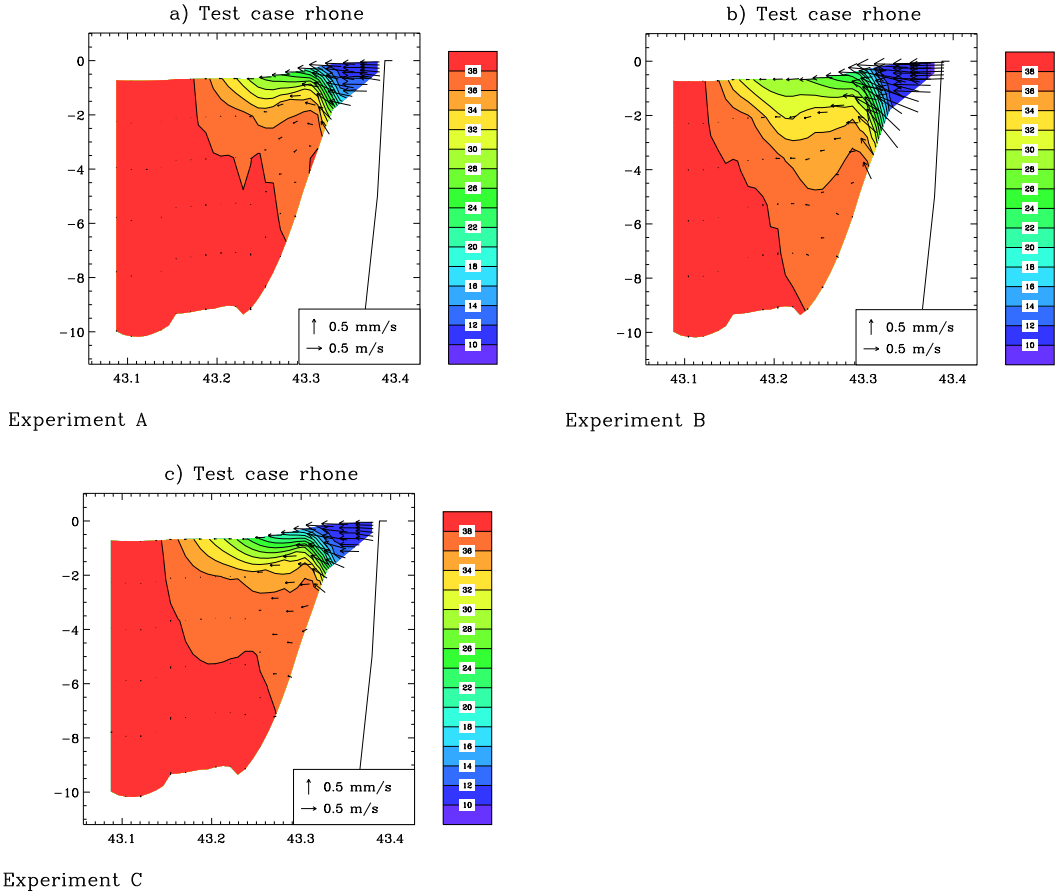

Figure 25.14: Test case ***rhone***. Distribution of currents and salinity along a vertical transect at 4.85^0E through the river mouth for experiment ***A*** (a), ***B*** (b), ***C*** (c).

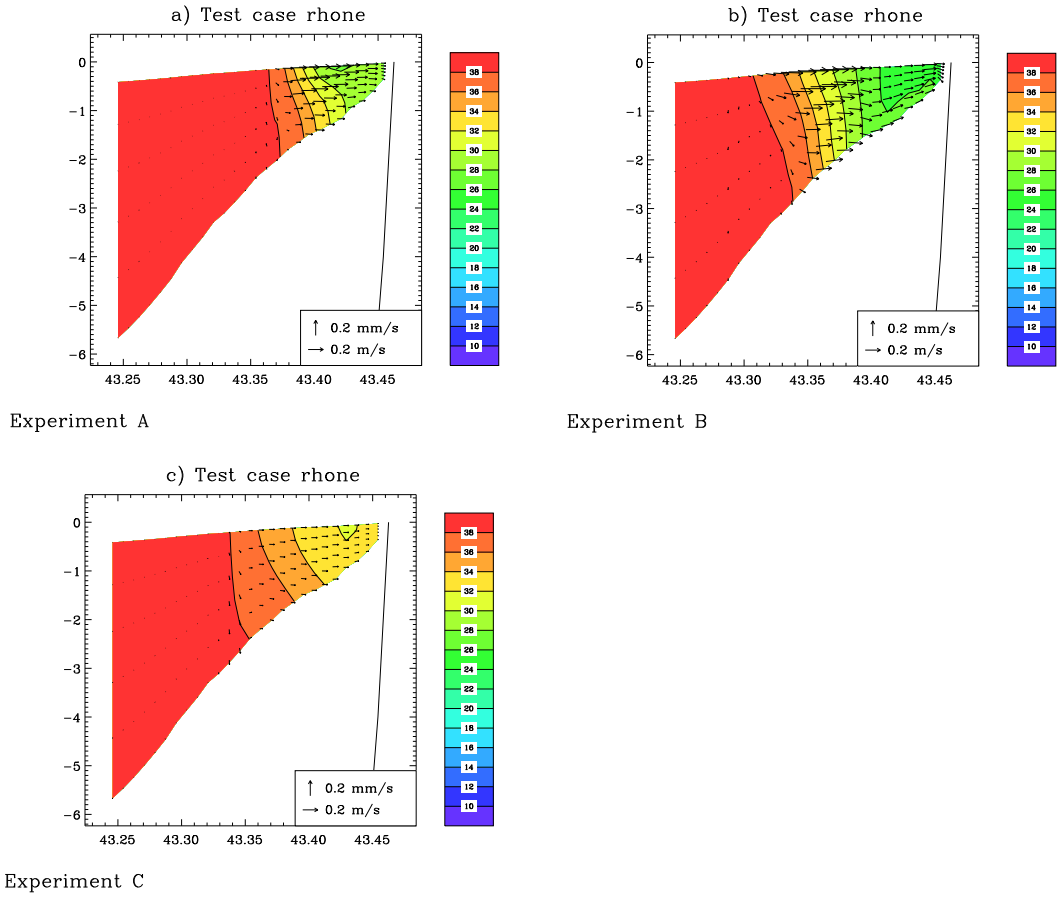

Figure 25.15: Test case ***rhone***. Distribution of currents and salinity along a vertical transect at 4.45^0E for experiment ***A*** (a), ***B*** (b), ***C*** (c).

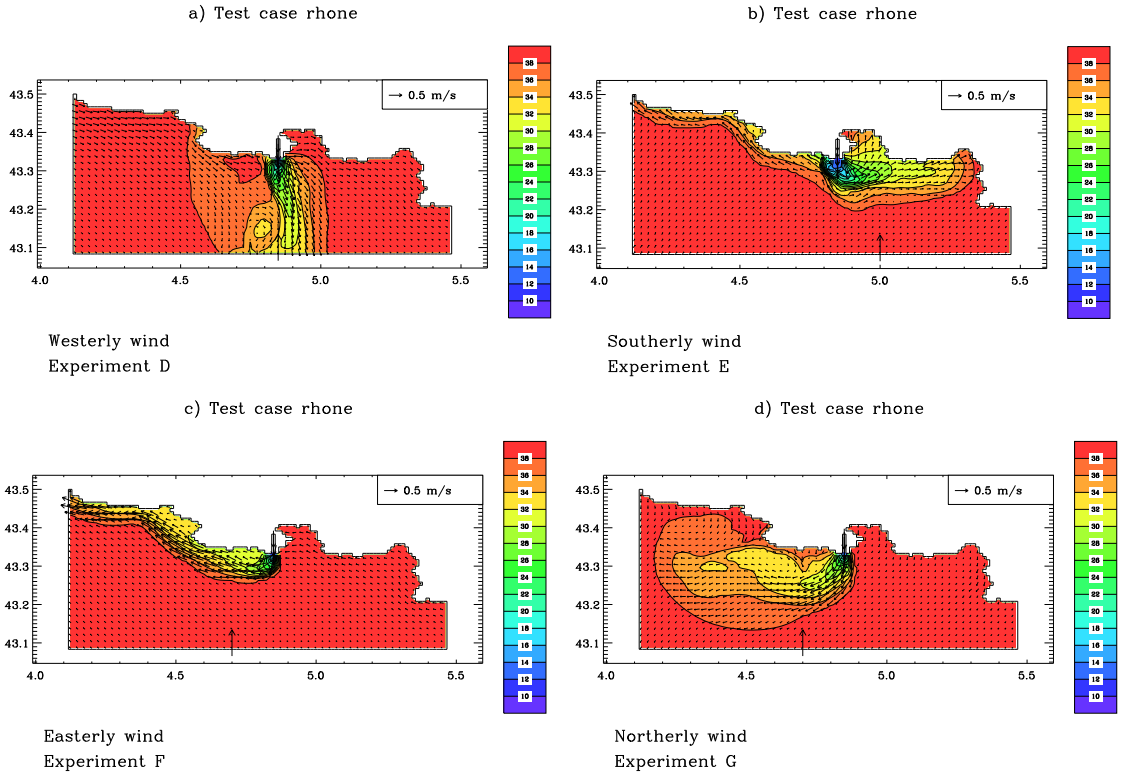

Figure 25.16: Test case ***rhone***. Surface distributions for salinity and currents for experiment ***D*** (a), ***E*** (b), ***F*** (c), ***G*** (d). The arrow on the southern boundary locates the position of the South-North transects shown in Figures 25.17.

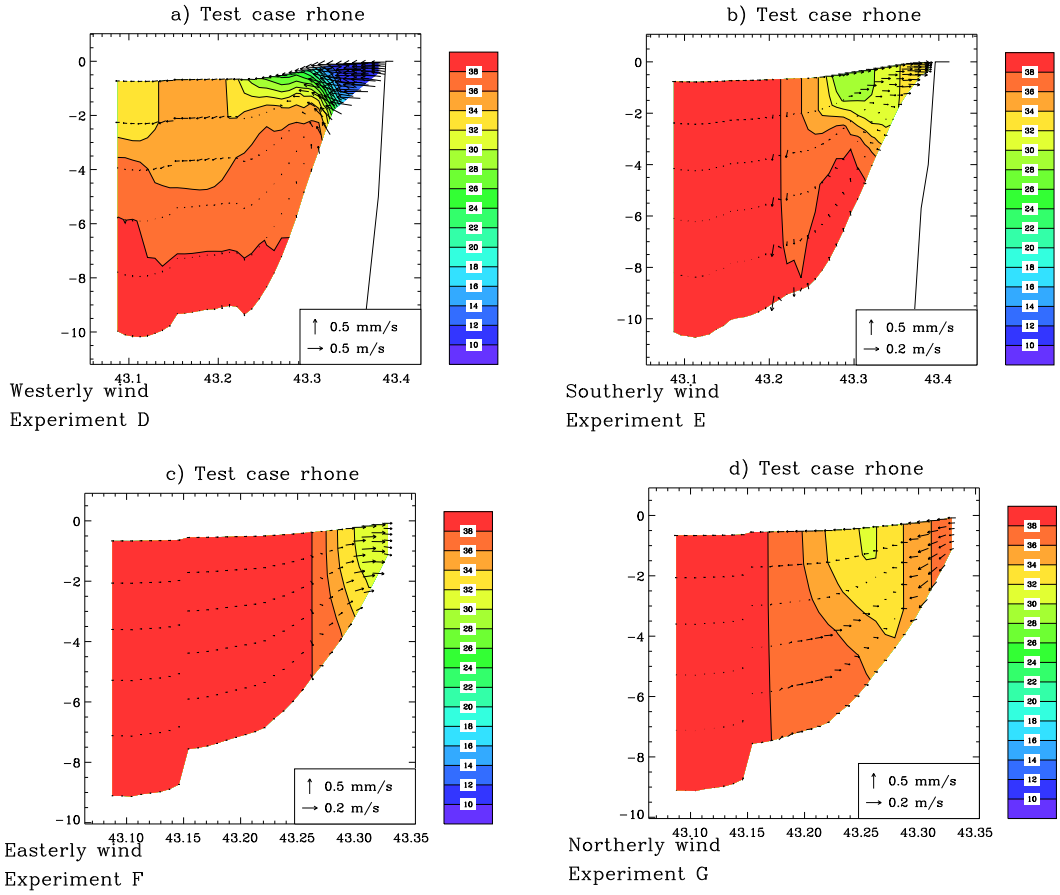

Figure 25.17: Test case ***rhone***. Distribution of currents and salinity along a vertical transect for experiment ***D*** at 4.85^{0}E (a), ***E*** at 5^{0}E (b), ***F*** at 4.7^0 (c) and ***G*** at 4.7^{0}E (d).

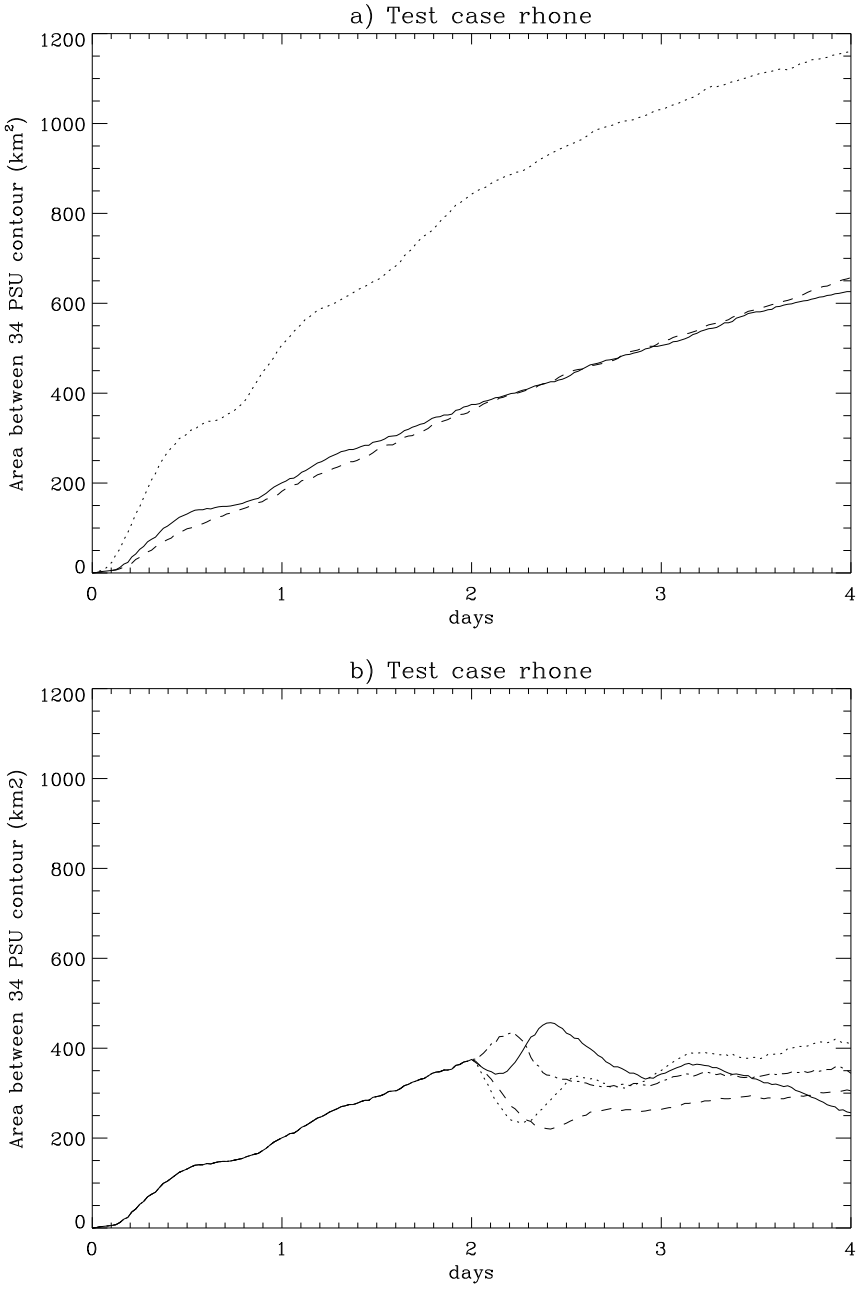

Figure 25.18: Test case ***rhone***. Plume area as defined as the area between the coast and the 34 PSU contour line: (a) experiment ***A*** (solid), ***B*** dots), ***C*** (dashes); (b) experiment ***D*** (solid), ***E*** (dots), ***F*** (dashes), ***G*** (dash-dots).

anti-cyclonically around a central bulge until the fresh water reaches the coast where it turns cyclonically to form a narrow coastal jet current. The transect through the river mouth (Figure 25.14a) shows a vertically uniform outflow, also due to the imposed zero baroclinic current at the river boundary. The region in front of the mouth is characterised by a strong horizontal salinity front and the formation of a shallow halocline of ∼2 m due to upwelling motions at the mouth. In the coastal plume the transport is onshore while no halocline is seen due to vertical mixing and the shallowness of the area (Figure 25.15).

- In experiment ***B*** the discharge rate is increased by a factor four. The results are qualitatively similar to the previous case, but the dimensions of the plume (extent of the bulge and width of the coastal plume) and the magnitude of the currents are now larger. The total plume area is 2 to 4 (depending on the criterion) times larger than the one in the previous (reference) case.
- Experiment ***C*** uses the Pacanowski-Philander turbulence model, which is more diffusive than the default RANS model taken in all other experiments. Currents and salinity fronts are almost the same near the mouth and the dimensions of the bulge are similar to the reference case. Vorticity is weaker within the two eddies. The jet current, plume fronts and onshore transports within the coastal plume are now much weaker. However, the total size of the plume remains the same (Figure 25.18a) since the slower advance of the coastal front, seen in Figure 25.13c, is compensated by a larger width of the plume (measured by the parameter d34max).

2. Wind experiments.
   Outside the surface plume, the direction of the surface flow is determined by surface and bottom friction. In the shallow parts where the surface current "feels" the bottom friction, the current flows predominantly in the direction of the wind. In the deeper parts the surface current turns to the right by Ekman drift. Within the plume the wind- and plume-driven currents interact in a more complex way. As can be seen in Figures 25.16 and is known from satellite images, the wind has a large impact on size and direction of the plume. Each experiment is further discussed below.

   - A westerly wind is imposed in experiment ***D***. Since the coast is located to the left of the wind direction, this case is known as

an upwelling favourable wind whereby the wind-driven circulation consists of an offshore (onshore) flow in the surface (bottom) layer and upwelling at the coast. Since wind- and plume-driven circulations act in the same sense at the mouth, the result, seen in Figure 25.17a, is a (slight) enforcement of the current magnitude. Main effect is that no bulge is formed and most fresh water is transported southwards with only a small Ekman deflection in the deeper areas near the southern boundary. This is the only experiment where fresh water is directly transported beyond the shelf and into the Gulf of Lions.

- A southerly onshore wind is taken in experiment ***E***. The results are manifestly different from the reference and previous cases. The onshore flow strongly inhibits the outflow of fresh water so that an even stronger lateral density front is formed close to the mouth. The bulge is still visible, but strongly deflected to the right at its southern edge where water depths are larger. The result is a coastal plume to the East of the mouth, extending into the Gulf of Fos, while a smaller plume remains to the West. The lateral density fronts within these plumes are less intense due to wind-induced turbulence and diffusion. This is also observed in Figure 25.17b .
- Experiment ***F*** represents the case of an easterly, downwelling favourable wind. The coast is now on the right of the wind direction giving an onshore (offshore) flow in the surface (bottom) layer and downwelling at the coast. The onshore surface transport limits the outward expansion of the plume and bulge. Since the alongshore wind-driven current is towards the West, the coastal jet current is strengthened. The coastal plume is driven towards the coast (as can be seen by inspecting the values of d34max) with stronger frontal gradients.
- When the wind arrives from the North (experiment ***G***), the wind-driven surface current is southwards near the coast and has a westward component in the deeper offshore areas. In analogy with the case of a northward wind in experiment ***E***, the bulge is now deflected to the West. Main difference with the no-wind case is the absence of a return flow towards the coast at the West of the bulge so that the plume becomes more and more detached from the coast. A consequence is the complete absence of a coastal plume. Within the detached plume, vertical stratification is reduced by wind mixing giving a deeper fresh water layer with a thickness of

$\sim$5 m (Figure 25.17d).